Journal of Ginseng Research 46 (2022) 225–234

Contents lists available at ScienceDirect

Journal of Ginseng Research

journal homepage: https://www.sciencedirect.com/journal/journal-of-ginseng-research

Research Article

The dehiscence process in *Panax ginseng* seeds and the stigmasterol biosynthesis pathway in terms of metabolomics

Jung Eun Min [a], Nguyen Phuoc Long [a], Ji Yeon Hong [a], Sun Jo Kim [a], Nguyen Hoang Anh [a], Daijie Wang [b], Xiao Wang [b], Jeong Hill Park [a], Sung Won Kwon [a, c, **], Seul Ji Lee [a, *]

[a] College of Pharmacy, Seoul National University, Seoul, Republic of Korea
[b] School of Pharmaceutical Sciences, Shandong Analysis and Test Center, Qilu University of Technology (Shandong Academy of Sciences), Jinan, China
[c] Plant Genomics and Breeding Institute, Seoul National University, Seoul, Republic of Korea

ARTICLE INFO

Article history:
Received 15 December 2020
Received in revised form
29 May 2021
Accepted 9 June 2021
Available online 15 June 2021

Keywords:
Dehiscence
Dormancy release
Ginseng seed
Squalene
Warm stratification

ABSTRACT

Background: Ginseng, officially known as *Panax ginseng* Meyer, has been traditionally used as a medicinal herb, particularly in Asia. Ginseng is propagated from seeds; however, seed germination is challenging, especially in its natural environment on farms. The seeds typically exhibit morphophysiological dormancy and require release from both morphological and physiological dormancy before germination. Although some studies have proposed methods for increasing seed germination rates, the underlying mechanisms of its dormancy release process remain unclear. Here, we investigated metabolic alterations during dehiscence in *P. ginseng* to determine their potential roles in dormancy release.
Methods: We compared the ginseng seed metabolome before and after dehiscence and the ginsenoside and phytosterol compositions of the seeds in both periods in the presence of related enzymes.
Results: After seed dehiscence, the sugar, amino acid, and squalene concentrations were significantly altered, phytosterols associated with the stigmasterol biosynthesis pathway were increased, while ginsenoside and brassinosteroid levels were not significantly altered. In addition, squalene epoxidase, cycloartenol synthase, 24-methylenesterol C-methyltransferase, and the stigmasterol biosynthesis pathway were activated.
Conclusion: Overall, our findings suggest that morphological activities that facilitate ginseng seed growth are the primary phenomena occurring during the dehiscence process. This study improves the understanding of *P. ginseng* germination processes and promotes further research of its germination and cultivation.

1. Introduction

Ginseng (*Panax ginseng* Meyer) is one of the most widely used medicinal herbs. Particularly, ginseng root has been reported to exert various therapeutic effects, such as anti-cancer potential, immune response enhancement, blood glucose level improvement, and insulin regulation [1–8]. Ginseng is propagated from seeds, which exhibit morphophysiological dormancy according to Baskin's classification theory [9]. Freshly harvested seeds have very thick and hard seed coats in addition to underdeveloped embryos with physiological dormancy. Consequently, a two-step dormancy release process, consisting of warm and cold stratification, is essential for seed germination. Generally, immediately after harvest, the seeds are stored in sand layers at 15–20°C for 3 months to allow warm stratification, followed by storage at 4°C for 3 months for cold stratification [10]. During warm stratification, the embryo begins to grow and the seed coat dehisces [11]. Therefore, the success of warm stratification can be confirmed by seed coat dehiscence. Dehiscence is splitting that occurs at maturity along a built-in line of weakness in a plant structure to release its contents. Although the morphological alterations that occur under dehiscence are known, their underlying molecular mechanisms or associated pathways remain unclear [12]. Investigating the underlying molecular activities during dehiscence may facilitate *P. ginseng* farming activities.

* Corresponding author.
** Corresponding author. College of Pharmacy, Seoul National University, Seoul 08826, Republic of Korea.
E-mail addresses: swkwon@snu.ac.kr (S.W. Kwon), dltmfwl2@snu.ac.kr (S.J. Lee).

https://doi.org/10.1016/j.jgr.2021.06.005

Metabolomics is an "omics" approach that aims to characterize all metabolites in a biological system. It can provide snapshots of an organism at a specific time point, which reflects the metabolic status [13,14]. Therefore, metabolomics is an appropriate method for investigating metabolic phenotypes. Untargeted metabolomics is applied in numerous fields, such as biomarker discovery, disease diagnosis and prognosis, and geographical discrimination of plants [15–20]. Among the most extensively applied metabolomics techniques, GC-MS is essential in plant metabolome research. GC-MS-based metabolomics can analyze volatile and non-volatile metabolites, particularly primary metabolic products. In addition, the retention indices and mass spectra are highly reproducible, and available mass spectra libraries can facilitate the putative identification of GC-MS spectral peaks with high confidence [21]. Most metabolomic and transcriptomic studies of ginseng have focused on the roots [22–24], whereas the seeds, which are essential for propagating this species, have not been widely examined.

In this study, we investigated the metabolic alterations during *P. ginseng* seed dehiscence and warm stratification. We identified and validated differentially expressed metabolites and predicted the pathways associated with dehiscence. We also investigated the phytosterol content and differential gene expression before and after dehiscence. Our results improve the understanding of the underlying mechanisms of dormancy release in *P. ginseng* and may lead to strategies for improving *P. ginseng* seed germination and cultivation.

2. Materials and methods

2.1. Plant materials

The *P. ginseng* seeds, harvested in July 2016, were provided by Gyeonggi Eastern Ginseng Nonghyup (Incheon, Korea). Seeds were stored at 14°C for 16 weeks for seed coat dehiscence. The seeds were checked every week, and wholly dehisced seeds were stored at −80°C until analyses.

2.2. Chemical reagents

Chloroform, methanol, water, methylene chloride, and methyl *tert*-butyl ether were purchased from JT Baker (Philipsburg, NJ, USA). Campesterol, β-sitosterol, clerosterol, Δ^5-avenasterol, lupeol, and 24-methylenecycloartanol were obtained from ChemFaces Biochemical Co., Ltd. (Wuhan, Hubei, China). Benzoic acid (d5) was purchased from Cambridge Isotope Laboratory (Andover, MA, USA). All other chemical reagents were obtained from Sigma Aldrich (St. Louis, MO, USA).

2.3. Untargeted metabolomics

Seed coats were removed to prevent potential contamination, after which the embryos and endosperms were ground in liquid nitrogen by a mortar and pestle and lyophilized. Next, 1 mL of chloroform:methanol:water (2:5:2) was added to each sample (35 mg). Samples were spiked with benzoic acid (d5) as an internal standard. The samples were vortexed and ultra-sonicated (Sonics & Material, Inc., Newtown, CT, USA) for 30 min at 40°C, followed by centrifugation at 16,000 × *g* for 5 min. The supernatants (600 μL) were removed for further analyses, and the remaining 300 μL of supernatants were used as quality control (QC) samples. The samples were dried under a nitrogen purge at 50°C, followed by the addition of anhydrous toluene (100 μL). The samples were then dried again under a nitrogen purge to eliminate all solvents, followed by derivatization. 100 μL of methoxyamine hydrochloride in pyridine (20 mg/mL) was added, and samples were incubated for 90 min at 30°C. Further, *N,O-Bis*(trimethylsilyl)trifluoroacetamide (100 μL) and trimethylchlorosilane (1%) were added and the samples were incubated again for 15 min at 70°C. The final 200-μL samples were analyzed by GC-MS.

The extracted samples were analyzed using a GC-mass spectrometer (Shimadzu-QP2010, Kyoto, Japan) with a DB-5MS column (30 m × 0.25 mm, 0.25 μm; Agilent Technologies, Santa Clara, CA, USA) to profile the ginseng seed metabolites. An injection with volume 1 μL and split mode with a 5:1 ratio was used. The injection temperature was 300°C. Helium was used as a carrier gas with a flow rate of 1 mL/min. The initial oven temperature was maintained at 70°C, then increased to 150°C at a rate of 5°C/min, 250°C at a rate of 8°C/min, 300°C at a rate of 5°C/min, and finally, held at 300°C for 10 min. The electron impact ionization method was used as a MS detector with 70 eV of electron energy, and mass data were collected using a scan mode of 30–600 *m/z*.

2.4. Phytosterol content analysis

Oil extraction and preparation of unsaponifiable fractions were performed according to previously described methods [25]. Briefly, 5 g of ginseng seed powder was boiled thrice under reflux in 50 mL of methylene chloride for 2 h. After filtering, the extract was concentrated by rotary vacuum evaporation. One gram of the obtained oil was added to 20 mL of 1 M KOH in methanol, and 1 mL of 0.1% (w/v) 5α-cholestane in methyl *tert*-butyl ether was added as an internal standard and stirred overnight. Subsequently, the mixture was diluted with 40 mL of distilled water and then extracted thrice with 30 mL methyl *tert*-butyl ether. Thereafter, 15 mL of 0.5 M KOH in methanol was added to the collected organic extract, and the solution was washed with 30 mL of distilled water until its pH became equivalent to the pH of the water, followed by a final wash with 15 mL of saturated sodium chloride solution. The solvent was eliminated by rotary vacuum evaporation.

Approximately 15 mg of the unsaponifiable fraction was subjected to the above derivatization step and analyzed with the same GC-MS instrument. The initial oven temperature was held at 190°C for 2 min, increased to 260°C at a rate of 5°C/min, 275°C at a rate of 5°C/min, 300°C at a rate of 5°C/min, and held at 300°C for 10 min. The other conditions were similar to those described above.

2.5. RNA extraction and real-time PCR analysis

Total RNA was extracted from ginseng seeds using an RNeasy RNA Plant Mini Kit (Qiagen, Hilden, Germany) according to the manufacturer's instructions. To eliminate genomic DNA, the samples were treated with RNase-Free DNase (Qiagen) before the final washing step. The quality and quantity of extracted RNA were measured using a NanoDrop ND-1000 spectrophotometer (Thermo Fisher Scientific, Waltham, MA, USA). For real-time PCR analysis, cDNA was synthesized from 1 μg of extracted RNA using M-MLV reverse transcriptase (Invitrogen, Carlsbad, CA, USA). The expression levels of different genes were determined using an AB 7300 Real-time PCR system (Applied Biosystems, Foster City, CA, USA) with PowerUp SYBR green master mix (Applied Biosystems) as the fluorescence reporter dye. The primer sequences of the target genes were SE (sense 5′-TCCTTTTTGGGTTCCTGCTC-3′, anti-sense 5′-GTATAAGCAAGAGCAGAGCCAGC-3′), cycloartenol synthase (CAS, sense 5′-GGGGAGTCTGCTTCACC-3′, anti-sense 5′-CTCCCCAACCAC-CAGAAG-3′), β-amyrin synthase (β-AS, sense 5′-TATCCTGGA-CACCGAAAGAAGG-3′, anti-sense 5′-GTAGTATGTCTTTCCAGCTGCCG-3′), dammarenediol synthase (DDS, sense 5′-GCATACCGCCGTTGAGATTA-3′, anti-sense 5′-TAGTGT-CAATCGTTCCGCTG-3′), 24-methylenesterol C-methyltransferase (SMT2, sense 5′-CTCTGCGAGGTGGTTCG-3′, anti-sense 5′-

GTCACCCACTCGTACGATAC-3′), 9-*cis*-epoxycarotenoid dioxygenase (sense 5′-CTTGTATGACTCCAGCGGAC-3′, anti-sense 5′-TATTCACCATCCCTGCCTCT-3′), and glyceraldehyde 3-phosphate dehydrogenase (GAPDH, sense 5′-GTGGCCAGAGTGGCTTTG-3′, anti-sense 5′-GACCGTGACTGGCTTCTCAC-3′).

2.6. Data preprocessing and compound identification

Raw data were first converted to *.cdf files using GC-MS PostRun v.4.11 (Shimadzu, Kyoto, Japan). The *.cdf files were then converted into *.abf format files using the Reifycs Analysis Base File converter (Reifycs, Inc., Tokyo, Japan). Next, the files were processed using MS-DIAL v.2.82 [26]. The data collection parameters were as follows: retention start time of 5 min, retention end time of 48.50 min, mass range start of 30 Da, and mass range end of 600 Da. For peak detection, a linear weighted moving average with a level of 2 scans was applied for peak smoothing, average peak width was 5 scans, and the minimum peak height was 2000 amplitude. For deconvolution parameters, the sigma window value and electron ionization were 0.5 and 10 amplitudes, respectively. Peak alignment was processed using one QC file as a reference file, and other parameters were set as to their defaults.

The deconvoluted spectra were imported into MS Search (version 2.2) coupled with the NIST14 library for compound identification. Primarily, a match score of 700 was utilized as the threshold for putative identification. The retention index, peak patterns in the spectrum, and reverse match score were also considered during the annotation process. The identities of differentially expressed metabolites, when applicable, were further confirmed by comparison with authentic commercial standards.

2.7. Exploration of data analysis and visualization

All metabolomics-related analyses were completed in MetaboAnalyst 4.0 [27]. Processed spectral data were log-transformed and scaled using the Pareto scaling method before actual analyses. Principal component analysis (PCA) and heatmap analysis were applied for data exploration and visualization. In addition, k-means clustering was used to obtain a first impression of the potential groupings of ginseng seeds before and after dehiscence.

2.8. Statistical analysis

In univariate analysis, *t*-test was used to detect differentially expressed metabolites between the non-dehisced and dehisced seed groups. In multivariate analysis, partial least squares discriminant analysis (PLS-DA) with cross-validation was conducted to develop a descriptive model of the separation between the two groups. All metabolites that differed significantly between the two groups in the *t*-test and had a variable importance in projection score of 1.2, were selected to develop a bio-signature of dehiscence.

Other statistical analyses were performed using SPSS Statistics 25 software (SPSS, Inc., Chicago, IL, USA). Continuous variables are presented as the mean ± standard deviation. A strict cut-off of adjusted P-value, false discovery rate of 0.001, was utilized as the significance level for metabolomics experiments. The false discovery rate was adopted by considering multiple comparisons, which is a characteristic of high-dimensional analyses. The discriminant capacity of the bio-signature was validated using an independent set of samples based on receiver operating characteristic curve analysis using the PLS-DA algorithm. A P-value of 0.05 was applied for all other analyses, unless otherwise stated.

2.9. Functional enrichment analysis

Pathway enrichment analysis of the differentially expressed metabolites was performed in MBRole version 2.0. Functional data for the compounds were obtained from the Kyoto Encyclopedia of Genes and Genomes database [28].

3. Results

3.1. Differentially expressed metabolites before and after seed dehiscence

Overlaid chromatograms revealed clear patterns in the peaks from different samples. However, the intensities of some peaks were quite distinct between the two groups. PCA was performed to visualize the metabolite profiles of samples and differences between the two groups before and after dehiscence (Fig. 1a). All 20 samples and seven quality control samples were separated on the PCA plot. Well-clustered QC samples and their low deviation values indicated the reliability of these experimental results. In addition, according to the results of heatmap analysis, the metabolite expression patterns significantly differed between the two groups (Fig. 1c). The K-means clustering results also demonstrated that the two groups of samples were effectively categorized (Additional file 1: Fig. S2).

t-Test and PLS-DA were performed on the same datasets; according to the *t*-test results, 72 metabolites exhibited significant changes after seed dehiscence, with 29 metabolites showing increases and 43 metabolites showing decreases (false discovery rate < 0.001). The descriptive model based on PLS-DA also effectively classified the two seed groups. Accuracy, R^2, and Q^2 were close to the optimal values, suggesting a distinction between the two groups (Fig. 1b). Twenty-three metabolites showed variable importance in projection scores greater than 1.2; 15 metabolites were identified as biomarkers of before and after seed dehiscence, which were amino acids, sugars, and their derivatives (Table 1).

To validate the metabolites as biomarkers of seed dehiscence, receiver operating characteristic curve analysis was performed on another set of experimental results using new samples and based on the same sample treatment and study design. This curve analysis based on the new dataset and 15 predicted biomarkers confirmed that the two seed groups were well-differentiated (Fig. 2a), and the area under the curve results indicated that they were suitable biomarkers for ginseng dehiscence (Fig. 2b). The heatmap derived from hierarchical clustering analysis also revealed that the two groups had distinct metabolite profiles (Fig. 2c).

3.2. Pathway enrichment analysis suggests squalene is crucial in ginseng seed dehiscence

The 15 metabolites identified as potential biomarkers were subject to pathway enrichment analysis to predict the potential metabolic pathways associated with seed dehiscence. Metabolic pathways associated with only 9 metabolites were identified (Table 2). These 9 metabolites are potentially involved in various metabolic pathways. For example, L-valine, L-leucine, and L-isoleucine were associated with seven different pathways, whereas squalene and *myo*-inositol were only associated with “biosynthesis of secondary metabolites” and “metabolic pathways.” In particular, squalene is a precursor of ginsenosides, the primary pharmacological ingredient in ginseng and a plant steroid essential for plant growth. Squalene dynamics may facilitate our understanding of the underlying molecular mechanisms of seed dehiscence.

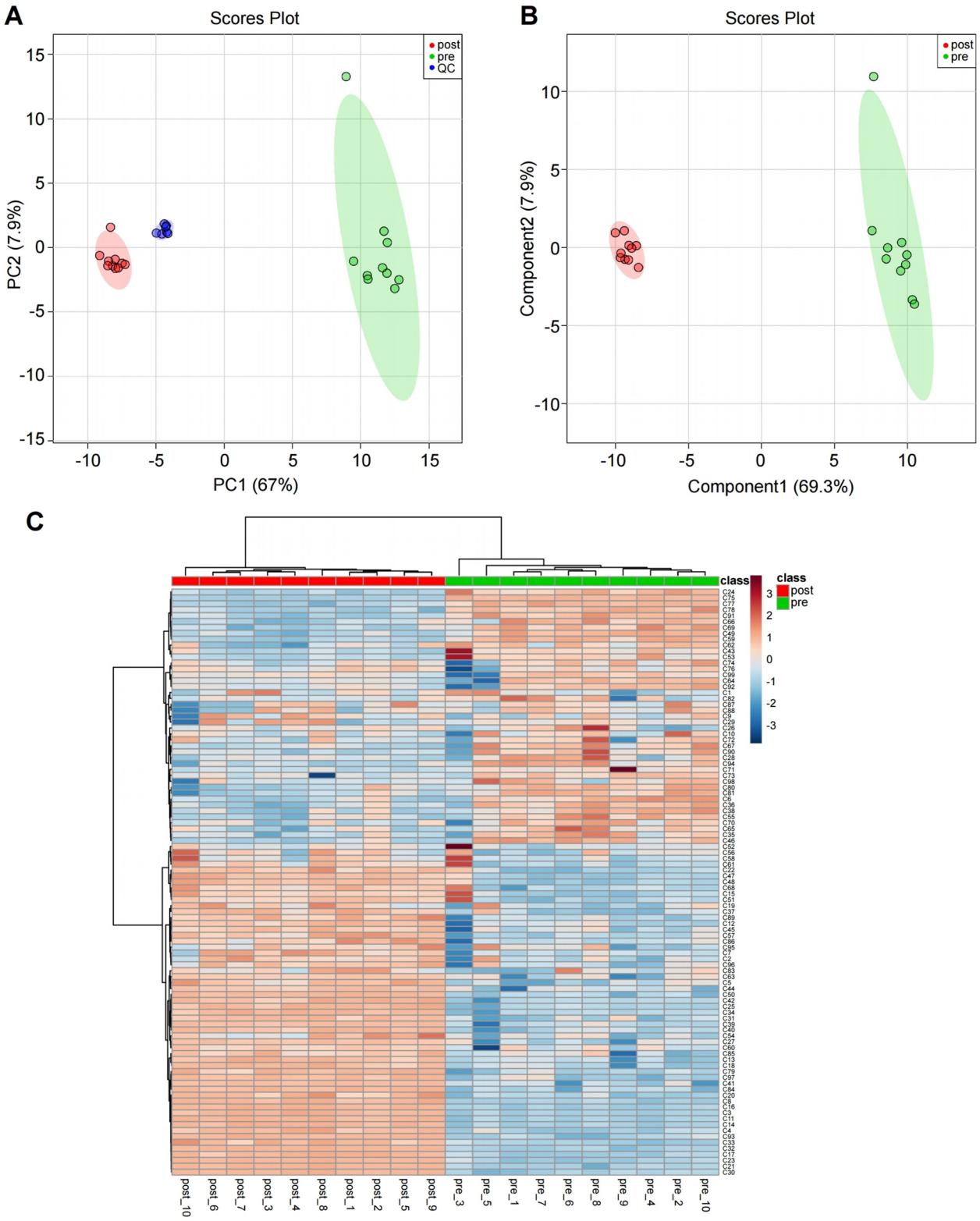

Fig. 1. Score plot of principal component analysis (PCA) (a), score plot of partial least squares discriminant analysis (PLS-DA) (b), and heatmap visualization (c) of before and after seed dehiscence. Red represents after dehiscence, green represents before dehiscence, and blue represents quality control (QC) samples. In the heatmap, "Cn" denotes the detected peaks.

Table 1
Differentially expressed metabolites before and after ginseng seed dehiscence.

Compound name	Compound number	Retention time (min)	Changes after dehiscence	VIP Score	Assign method
L-Valine-TMS	C3	6.66	Increase	1.35	Standard
2-Aminobutyric acid	C8	8.55	Increase	1.23	Standard
L-Valine-2TMS	C11	9.62	Increase	1.34	Standard
L-Leucine	C14	11.07	Increase	1.36	Standard
L-Isoleucine	C16	11.6	Increase	1.31	Standard
L-Serine	C21	13.37	Increase	1.67	Standard
L-Threonine	C23	13.97	Increase	1.75	Standard
Glutaric acid	C24	14.58	Decrease	1.44	Standard
L-5-Oxoproline	C32	17.3	Increase	1.34	Library
L-Asparagine-2TMS	C39	18.91	Increase	1.27	Standard
L-Phenylalanine	C41	19.32	Increase	1.73	Standard
L-Asparagine-3TMS	C42	20.14	Increase	1.42	Standard
Tyrosine	C50	23.42	Increase	1.38	Standard
D-Trehalose	C75	33.33	Decrease	1.81	Library
D-*myo*-Inositol	C77	33.94	Decrease	1.48	Library
Squalene	C78	34.39	Decrease	1.26	Standard
Galactinol	C84	36.18	Increase	1.87	Library

3.3. Comparison of plant steroid composition

Plant steroids, including phytosterols and brassinosteroids (BRs), are synthesized from squalene. Thus, a decrease in squalene after seed dehiscence may influence the composition of the seed oil. Therefore, the unsaponifiable fraction in the seed oil before and after ginseng seed dehiscence was compared using GC-MS (Fig. 3) and 12 phytosterols were identified using a combination of the retention order and mass fragmentation data or authentic standards based on references [29,30] (Table 3).

The retention order and mass fragmentation patterns were compared with those determined in a similar previous study that analyzed American ginseng seed oil [25], revealing that peaks 8, 10, 11, and 12 were assigned tentatively as $\Delta^{5,24(25)}$-stigmasterol, Δ^{7}-avenasterol, 24-methylenecycloartanol, and citrostadienol, respectively. Peaks 1–7 and 9 were confirmed as squalene, 2,3-oxidosqualene, campesterol, stigmasterol, clerosterol, β-sitosterol, Δ^{5}-avenasterol, and lupeol, respectively, by comparing the retention times and mass spectra of their authentic standards. The 8 phytosterols identified using standards were analyzed quantitatively, and 2,3-oxidosqualene was found to be a major component of ginseng seed oil, followed by squalene and Δ^{5}-avenasterol. Based on the comparison of the pre- and post-dehiscence groups, 2,3-oxidosqualene, Δ^{5}-avenasterol, and stigmasterol increased significantly after dehiscence, whereas squalene and lupeol decreased after dehiscence; however, campesterol, clerosterol, and β-sitosterol exhibited no significant differences (Table 4).

Because the amounts of Brassinolide (BL) in plants are often very low, it was analyzed in the unsaponifiable fraction of ginseng seed oil as a derivative of bismethaneboronate using GC-MS-selective ion monitoring. Bismethaneboronate BL (BL-BMB) ions were observed at *m/z* 528, and their mass fragmentation is shown in Additional file 1: Fig. S3. Please consider using the following summarized alternative that I have provided below:

“We analyzed fragment ions of BL-BMB in ginseng seeds at m/z 155, 177, and 374, based on a previous study which identified abundant fragment ions at these three values BL-BMB using GC-electrospray ionization-MS [31]. The peak areas of BL-BMB did not vary between non-dehisced and dehisced seeds, suggesting BL was not altered during dehiscence.

Analysis of the plant steroid composition revealed that phytosterols showing increases following seed dehiscence belong to the stigmasterol biosynthesis pathway (Fig. 4), also indicating that stigmasterol biosynthesis is activated during warm stratification.

3.4. Differential expression of enzymes based on real-time PCR

To confirm that the stigmasterol biosynthesis pathway is activated mainly during warm stratification, SE, CAS, β-AS, DDS, and SMT2 were compared between pre- and post-dehiscence seeds. According to Qi et al [32], 9-*cis*-epoxycarotenoid dioxygenase increased significantly after warm stratification and is a positive control for seed dehiscence. According to the results of real-time PCR, SE, CAS, and SMT2 expression increased significantly after seed dehiscence, whereas β-AS expression was not altered. In addition, DDS was undetectable both before and after seed dehiscence (Fig. 5).

4. Discussion

Panax ginseng seeds typically exhibit morphophysiological dormancy, indicating that they require both morphological and physiological dormancy release before germination can occur. These releases take place in the form of warm stratification, known as dehiscence, followed by cold stratification. The dehiscence process is crucial for the cultivation of ginseng because it can take more than 18 months to germinate ginseng seeds if the dehiscence process does not occur appropriately after seeds are stored in the sand for 3 months at 15–20°C [11,33]. Therefore, various studies have attempted to develop strategies for increasing ginseng seed dehiscence rates. For instance, Yang et al [34] reported that treatment with gibberellin enhances seed dehiscence rates compared to warm stratification exclusively. In addition, increasing gibberellic acid (GA_3) concentrations can increase seed dehiscence rates [35,36]. Furthermore, treatment of ginseng seeds with kinetin in combination with GA_3 can increase dehiscence rates to 96.2%, compared with a rate of 90.6% in seeds exposed to warm stratification alone [12]. In a previous study of American ginseng (*Panax quinquefolius* L.) seeds, 25,190 genes were compared by transcriptomic analysis based on Kyoto Encyclopedia of Genes and Genomes pathway annotation in digital gene expression libraries. Enrichment pathway analysis revealed pathways potentially associated with seed dormancy releases, such as steroid biosynthesis, flavonoid biosynthesis, flavone and flavonol biosynthesis, and starch and sucrose metabolism [32]. Transcriptomic analysis on *Panax notoginseng* (Burk) F.H. Chen seeds revealed 78 differentially expressed genes associated with seed dormancy; of these, 15 genes were involved in the abscisic acid and GA_3 pathways [37].

In the current study, by comparing the metabolome of *P. ginseng* seeds before and after dehiscence, we found that amino acids and

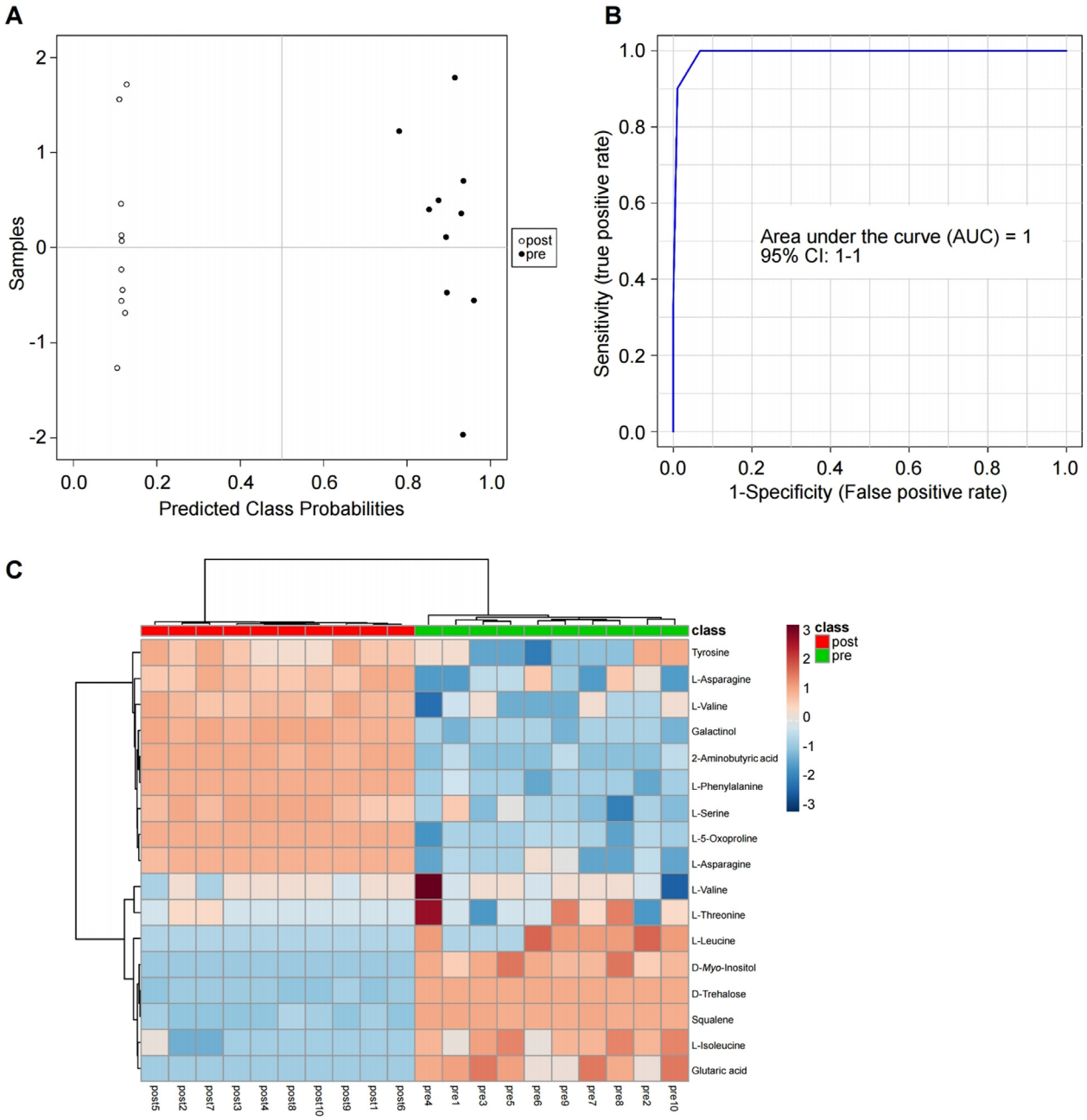

Fig. 2. Specificity and sensitivity of identified metabolites as biomarkers. Class distribution (a), receiver operating characteristic (ROC) curve analysis (b), and heatmap analysis (c) revealed a distinction before and after seed dehiscence.

Table 2
Metabolic pathways[a] involving identified Metabolites predicted as dehiscence biomarkers.

	L-Valine	L-Leucine	L-Isoleucine	L-Serine	L-Threonine	L-Asparagine	Tyrosine	*myo*-Inositol	Squalene
Aminoacyl-tRNA biosynthesis	O	O	O	O	O	O	O	-	-
Valine, leucine, and isoleucine biosynthesis	O	O	O	-	O	-	-	-	-
ABC transporters	O	O	O	O	O	-	-	-	-
Biosynthesis of secondary metabolites	O	O	O	O	O	O	O	O	O
Glucosinolate biosynthesis	O	O	O	-	-	-	O	-	-
Valine, leucine, and isoleucine degradation	O	O	O	-	-	-	-	-	-
Cyanoamino acid metabolism	-	-	-	O	-	O	-	-	-
Metabolic pathways	O	O	O	O	O	O	O	O	O

[a] Pathway related to 2-aminobutyric acid, glutaric acid, L-5-oxoproline, L-phenylalanine, D-trehalose, and galactinol was not identified. O: compounds in the pathway.

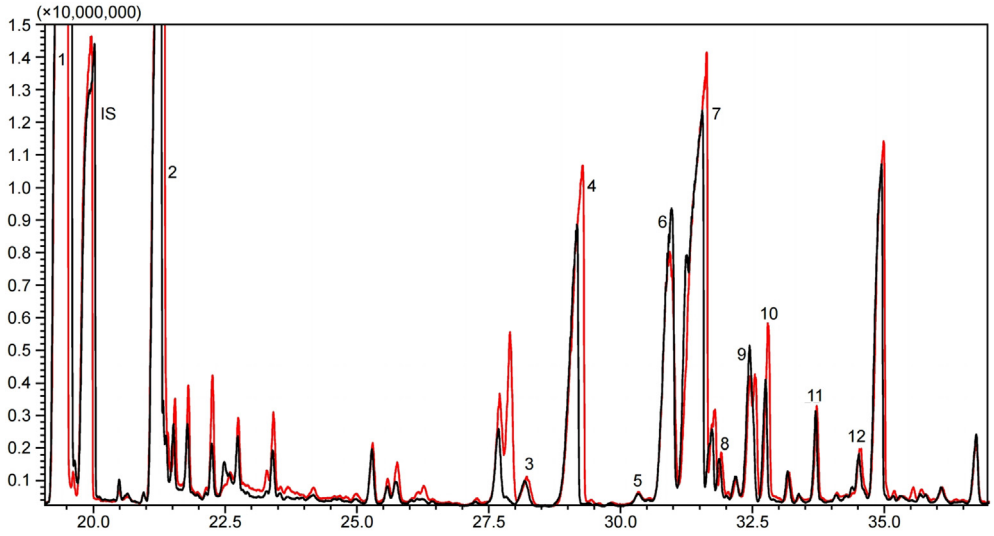

Fig. 3. Overlaid GC-MS chromatogram of phytosterol fractions before (black) and after (red) *Panax ginseng* seed dehiscence. 5α-Cholestane was used as the internal standard (IS). Identified peaks are listed in Table 3.

Table 3
Fragmentation ions for identification of phytosterols in *Panax ginseng*

Peak	Compound	Fragmentation ions, *m/z* (RI)[a]					
		M+	M-15	M-90	M-105	M-129	others
1	Squalene	410 [1]					367 [1], 341 [2], 231 [1], 203 [2], 189 [2], 149 [11], 137 [18], 136 [20], 123 [14], 121 [19], 109 [13], 107 [12], 95 [27], 93 [16], 82 [11], 81 (93), 69[b]
2	2,3-Oxidosqualene	426 [1]					357 [1], 231 [1], 203 [3], 191 [2], 149 [9], 135 [22], 133 [7], 123 [14], 121 [17], 109 [18], 107 [19], 95 [28], 93 [25], 81 (90), 71 [50], 69[b]
3	Campesterol	472 [19]	457 [5]	382 [47]	367 [23]	343 [47]	315 [3], 255 [14], 145 [31], 129[b]
4	Stigmasterol	484 [20]	469 [3]	394 [23]	379 [8]	355 [8]	343 [4], 255 [26], 213 [8], 145 [19], 133 [21], 129 [53], 97 [20], 95 [19], 83[b]
5	Clerosterol	484 [33]	469 [8]	394 [25]	379 [11]	355 [16]	386 [6], 379 [11], 355 [16], 296 [11], 255 [13], 213 [13], 139 [30], 129 (88), 119 [38], 107 [35], 81 [48], 55[b]
6	β-Sitosterol	486 [25]	471 [7]	396 [52]	381 [20]	357 [47]	394 [25], 255 [15], 213 [9], 145 [29], 129[b], 95 [40], 73 [50]
7	Δ^5-Avenasterol	484 [6]	469 [5]	394 [3]	379 [5]	355 [5]	386 (79), 296 (68), 281 [45], 257 [24], 255 [14], 129[b], 95 [47], 55 (94)
8	$\Delta^{5,24(25)}$-Stigmasterol	484 [11]	469 [5]	394 [6]	379 [7]	355 [4]	386 [43], 343 [9], 296 [39], 281 [26], 257 [14], 255 [11], 253 [17], 129 (73), 121 [26], 119 [40], 107 [32], 105 [29], 97 (68), 95 [37], 93 [31], 81 [40], 75 [42], 73 (72), 69 (67), 55[b]
9	Lupeol	498 [16]	483 [7]	408 [11]	393 [13]	369 [13]	279 [12], 218 [31], 203 [41], 190 [53], 189 (75), 136 [45], 135 (64), 123 [45], 121 (64), 109 (94), 107 (65), 95 (92), 93 (61), 81 (71), 75 (75), 73[b]
10	Δ^7-Avenasterol	484 [2]	469 [6]	394 [1]	379 [4]		386 [41], 371 [6], 343[b], 296 [7], 281 [9], 253 [27], 145 [18], 119 [17]
11	24-Methylenecycloartanol	512 [1]	497 [3]	422 [40]	407 [38]		379 [54], 353 [15], 300 [9], 147 [41], 135 (61), 121 [55], 109 (60), 107 (62), 105 [44], 95 (83), 81 [58], 73[b]
12	Citrostadienol	498 [2]	483 [4]	408 [2]	393 [6]		400 [51], 357[b], 267 [27], 145 [21], 133 [22]

[a] Relative intensity compared to base peak (percent).
[b] Base peak (relative intensity = 100 %).

sugars were significantly altered. Freshly harvested ginseng seeds have an undeveloped embryo [33]. Therefore, during warm stratification, changes in amino acid and sugar concentrations as well as composition may be associated with embryogenesis of the ginseng seed. Indeed, similar physiological phenomena, which are strongly associated with starch and protein accumulation, have been reported in *Arabidopsis thaliana* and *Theobroma cacao* L. seeds [38,39]. Furthermore, numerous enzymes associated with the biosynthesis of plant steroids in ginseng have been reported [40,41]. As illustrated in Fig. 4, squalene epoxidase converts squalene into 2,3-oxidosqualene. The 2,3-oxidosqualene is converted into three significant compounds, cycloartenol, β-amyrin, and dammarenediol by CAS, β-AS, and DDS, respectively. Cycloartenol is one of the precursors of phytosterols. Oleanane-type triterpene saponins originate from β-amyrin. In addition, dammarenediol is an essential precursor of dammarane-type triterpene saponins. Following activation of the biosynthetic pathway by CAS, a large amount of intermediate 24-methylenelophenol is formed. The biosynthetic pathway can induce divergence in phytosterol synthesis. When C4-demethylase is activated, it becomes episterol, which is the precursor of BL. Additionally, 24-ethylidenelophenol, the precursor of stigmasterol, is formed via methylation of 24-methylenelophenol through activation by SMT2 [42,43]. The squalene concentrations were notably decreased following seed dehiscence in the present

Table 4
Phytosterol contents before and after *Panax ginseng* seed dehiscence

Peak	Compound	Contents (mg per 100 g of seed oil, n = 3)	
		Before dehiscence	After dehiscence
1	Squalene*	166.05 ± 11.15	120.19 ± 21.08
2	2,3-Oxidosqualene*	362.75 ± 32.92	616.45 ± 47.45
3	Campesterol	1.85 ± 0.70	2.05 ± 0.33
4	Stigmasterol*	25.58 ± 4.00	48.91 ± 0.64
5	Clerosterol	1.37 ± 0.40	1.29 ± 0.42
6	β-Sitosterol	55.22 ± 2.25	58.72 ± 6.36
7	Δ^5-Avenasterol*	138.52 ± 6.68	170.71 ± 7.98
8	$\Delta^{5,24(25)}$-Stigmasterol	-	-
9	Lupeol*	14.86 ± 0.12	8.71 ± 0.64
10	Δ^7-Avenasterol	-	-
11	24-Methylenecycloartanol	9.26 ± 1.02	10.20 ± 0.92
12	Citrostadienol	-	-

* $P < 0.05$.

study. In the triterpene biosynthetic pathway in ginseng, squalene is converted into 2,3-oxidosqualene by SE, and 2,3-oxidosqualene is a precursor of two different types of ginsenosides, dammarene-type and oleanane type, in addition to phytosterols including BRs [44,45].

Ginsenosides are some of the most pharmaceutically active compounds in ginseng, and some studies have aimed to increase their concentrations in *P. ginseng* roots, with a primary focus on squalene. Overexpression of the squalene synthase gene increases the levels of downstream enzymes, including SE, CAS, β-AS, and DDS, which increase the ginsenoside and phytosterol concentrations [46]. In addition, Sivakumar et al [47] reported that exposing *P. ginseng* roots to exogenous squalene increased phytosterol as well as ginsenoside concentrations. Therefore, the alteration of the squalene concentrations in the present study suggests shifts in the ginsenoside or phytosterol concentrations. Ginsenosides were not

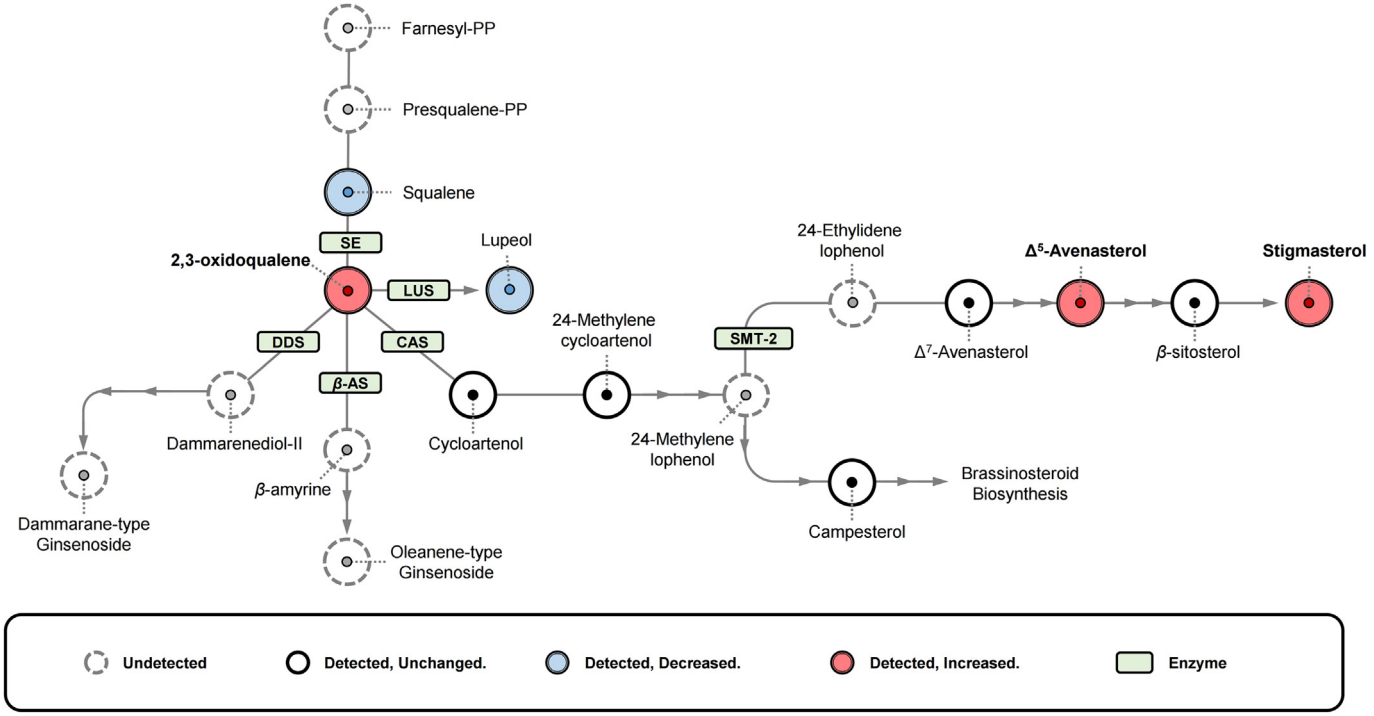

Fig. 4. Trends observed in phytosterol biosynthesis pathways. Red phytosterols increased, while blue phytosterols decreased after seed dehiscence.

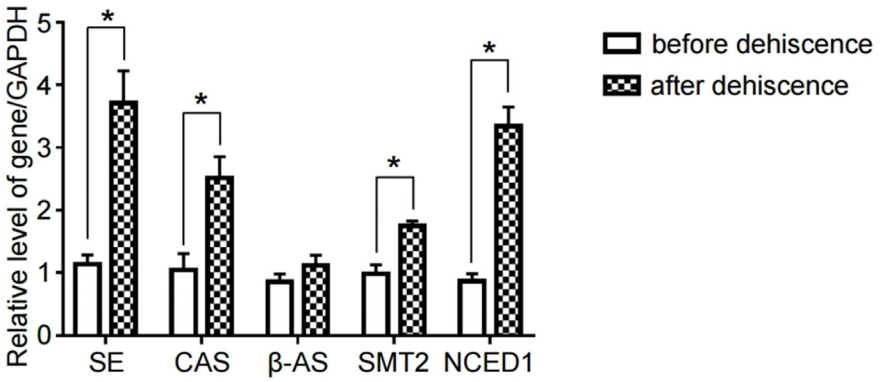

Fig. 5. Relative levels of expression of genes involved in the phytosterol and ginsenoside biosynthetic pathways. Asterisks indicate that the change in the gene after dehiscence was significant (P-value < 0.005). NCED1 was used as positive control for ginseng seed dehiscence.

observed before or after ginseng seed dehiscence using HPLC-UV-visible spectroscopy (data not shown). However, one of the end-products of phytosterol biosynthesis, stigmasterol, was increased significantly after ginseng seed dehiscence; in contrast, the concentrations of other end-products, campesterol and BL, were not altered. BL is the most biologically active brassinosteroid, is synthesized from campesterol [48]. Therefore, the presence of campesterol implies the presence of BL in ginseng seeds. Phytosterols are primary components of the cell membrane and facilitate cell fluidity and permeability, similar to other sterols. Phytosterol synthesis is increased during seed germination to meet the demands for new membranes and, with seed maturity, the rate of increase declines gradually. The roles of phytosterols in cellular proliferation and differentiation have also been determined. Although cholesterol alone restores growth by only 40–50% compared to that in the control, with stigmasterol alone, it is possible to achieve full growth [49,50].

Phytosterols can also regulate membrane-bound enzymes. For example, stigmasterol stimulates proton pumps in cellular membranes; therefore, it participates in some signal transduction activities associated with seed development [49–52]. Phytosterols are also precursors of several plant hormones, particularly BRs. It has been reported that BRs regulate cell elongation and differentiation. Consequently, BRs control seed germination, development, and tolerance to numerous stress factors [53–55]. BRs perform "cross-talk" with the key growth-regulating hormones GA_3 and abscisic acid (ABA). BR binding to BRI1 (BRASSINOSTEROID INSENSITIVE 1) leads to heterodimerization with BAK1 (BRASSINOSTEROID INSENSITIVE 1-ASSOCIATED RECEPTOR KINASE 1), and the dimer prohibits the ability of BIN2 (BRASSINOSTEROID INSENSITIVE 2) to phosphorylate BZR1/BES1 (BRASSINAZOLE RESISTANT 1/BRI1-EMS-SUPPRESSOR 1) [56]. Activated BZR1/BES1 can promote GA_3 biosynthesis and GA_3 degradation of DELLA proteins which then promote the repression of BZR1/BES1 activity. It has also been reported that BR and ABA negatively regulate each other [57]. Increased ABA levels upregulate BIN2, one of the primary negative regulators of BR signaling, and BR inhibits ABA activity through PP2C (protein phosphatase 2C) [58]. In a previous study, ABA levels increased during the dehiscence period in *P. ginseng* seeds and decreased discernably after dehiscence; GA_3 levels were not altered during dehiscence and increased after seed dehiscence [59]. The increased ABA levels may regulate BR levels during the seed dehiscence period, leading to no change in BR after seed dehiscence.

Our results demonstrate that metabolites are important factors in morphological growth changes during *P. ginseng* seed dehiscence. The results suggest that seed growth is the primary activity occurring under warm stratification, whereas other physiological changes, such as hormonal changes, may take place later. For germination in *P. ginseng* seeds, warm stratification followed by cold stratification is required. Therefore, to further enhance our understanding of the mechanisms of *P. ginseng* seed germination, additional in-depth investigations are warranted to determine the metabolic activities and alterations occurring during cold stratification.

5. Conclusions

The metabolite profiles of ginseng seeds before and after dehiscence were analyzed using gas GC-MS and compared to identify differentially expressed metabolites between the two groups. Sugar, amino acid profiles, and particularly squalene concentrations were altered after seed dehiscence. Phytosterols, which are precursor metabolites of squalene associated with seed growth, were increased after seed dehiscence. In addition, enzymes associated with phytosterol biosynthesis, SE, CAS, and SMT2, increased after seed dehiscence. Nevertheless, other secondary metabolites such as ginsenosides and BRs were potentially not associated with dehiscence. Overall, our results suggest that during *P. ginseng* seed dehiscence, morphological activities, particularly growth, are dominant.

Author contributions

SWK and JEM designed the study. JEM, NPL, JYH, SJK, and NHA performed chemical and biological experiments and analyzed and interpreted the data. SWK, JHP, and SJL interpreted the data. JEM, NPL, DW, and XW wrote the manuscript. All authors critically revised the manuscript and approved the final contents.

Declaration of competing interest

The authors claim that the researchers in this study have no conflicts of interest to declare.

Acknowledgments

This work was supported by the Rural Development Administration of Korea [PJ01420102]; BK21 Plus Program in 2021; the BioSynergy Research Project of the Ministry of Science, ICT and Future Planning through the National Research Foundation of Korea (NRF) [2012M3A9C4048796]; and Basic Science Research Program through the National Research Foundation of Korea (NRF) funded by the Ministry of Education [2019K1A3A1A05088041].

Appendix A. Supplementary data

Supplementary data to this article can be found online at https://doi.org/10.1016/j.jgr.2021.06.005.

References

[1] Lee DC, Lau AS. Effects of Panax ginseng on tumor necrosis factor-α-mediated inflammation: a mini-review. Molecules 2011;16(4):2802–16.
[2] Shergis JL, Zhang AL, Zhou W, Xue CC. Panax ginseng in randomised controlled trials: a systematic review. Phytotherapy Research 2013;27(7):949–65.
[3] Shin HR, Kim JY, Yun TK, Morgan G, Vainio H. The cancer-preventive potential of Panax ginseng: a review of human and experimental evidence. Cancer Causes & Control 2000;11(6):565–76.
[4] Vogler B, Pittler M, Ernst E. The efficacy of ginseng. A systematic review of randomised clinical trials. European Journal of Clinical Pharmacology 1999;55(8):567–75.
[5] Reay JL, Kennedy DO, Scholey AB. Single doses of Panax ginseng (G115) reduce blood glucose levels and improve cognitive performance during sustained mental activity. Journal of Psychopharmacology 2005;19(4):357–65.
[6] Reay JL, Kennedy DO, Scholey AB. Effects of Panax ginseng, consumed with and without glucose, on blood glucose levels and cognitive performance during sustained 'mentally demanding'tasks. Journal of Psychopharmacology 2006;20(6):771–81.
[7] Kang S, Min H. Ginseng, the'immunity boost': the effects of Panax ginseng on immune system. Journal of Ginseng Research 2012;36(4):354.
[8] Kim SW, Gupta R, Lee SH, Min CW, Agrawal GK, Rakwal R, et al. An integrated biochemical, proteomics, and metabolomics approach for supporting medicinal value of Panax ginseng fruits. Frontiers in Plant Science 2016;7(994).
[9] Baskin JM, Baskin CC. A classification system for seed dormancy. Seed Science Research 2004;14(1):1–16.
[10] Lee J-S, Lee S-S, Lee J-H, Ahn I-O. Effect of seed size and cultivars on the ratio of seed coat dehiscence and seedling performance in Panax ginseng. Journal of Ginseng Research 2008;32(3):257–63.
[11] Kwon W, Lee J, Lee M. Optimum chilling terms for germination of the dehisced ginseng (Panax ginseng CA Meyer) seed. J Ginseng Res 2001;25(4):167–70.
[12] Lee J-W, Jo I-H, Kim J-U, Hong C-E, Kim Y-C, Kim D-H, et al. Improvement of seed dehiscence and germination in ginseng by stratification, gibberellin, and/or kinetin treatments. Horticulture, Environment, and Biotechnology 2018;59(3):293–301.
[13] Patti GJ, Yanes O, Siuzdak G. Innovation: metabolomics: the apogee of the omics trilogy. Nature Reviews: Molecular Cell Biology 2012;13(4):263.

[14] Weckwerth W. Metabolomics in systems biology. Annual Review of Plant Biology 2003;54(1):669–89.
[15] Xia J, Broadhurst DI, Wilson M, Wishart DS. Translational biomarker discovery in clinical metabolomics: an introductory tutorial. Metabolomics 2013;9(2):280–99.
[16] Styczynski MP, Moxley JF, Tong LV, Walther JL, Jensen KL, Stephanopoulos GN. Systematic identification of conserved metabolites in GC/MS data for metabolomics and biomarker discovery. Analytical Chemistry 2007;79(3):966–73.
[17] Alonso A, Marsal S, Julià A. Analytical methods in untargeted metabolomics: state of the art in 2015. Frontiers in Bioengineering and Biotechnology 2015;3:23.
[18] Nguyen HT, Lee D-K, Choi Y-G, Min J-E, Yoon SJ, Yu Y-H, et al. A 1H NMR-based metabolomics approach to evaluate the geographical authenticity of herbal medicine and its application in building a model effectively assessing the mixing proportion of intentional admixtures: a case study of Panax ginseng: metabolomics for the authenticity of herbal medicine. Journal of Pharmaceutical and Biomedical Analysis 2016;124:120–8.
[19] Kim J, Jung Y, Song B, Bong Y-S, Lee K-S, Hwang G-S. Discrimination of cabbage (Brassica rapa ssp. pekinensis) cultivars grown in different geographical areas using 1H NMR-based metabolomics. Food Chemistry 2013;137(1–4):68–75.
[20] Quanbeck S, Brachova L, Campbell A, Guan X, Perera A, He K, et al. Metabolomics as a hypothesis-generating functional genomics tool for the annotation of Arabidopsis thaliana genes of “unknown function”. Frontiers in Plant Science 2012;3(15).
[21] Emwas A-HM. The strengths and weaknesses of NMR spectroscopy and mass spectrometry with particular focus on metabolomics research. Metabonomics 2015:161–93. Springer.
[22] Jayakodi M, Lee S-C, Lee YS, Park H-S, Kim N-H, Jang W, et al. Comprehensive analysis of Panax ginseng root transcriptomes. BMC Plant Biology 2015;15(1):138.
[23] Li X-J, Yang J-L, Hao B, Lu Y-C, Qian Z-L, Li Y, et al. Comparative transcriptome and metabolome analyses provide new insights into the molecular mechanisms underlying taproot thickening in Panax notoginseng. BMC Plant Biology 2019;19(1):451.
[24] Fan H, Li K, Yao F, Sun L, Liu Y. Comparative transcriptome analyses on terpenoids metabolism in field- and mountain-cultivated ginseng roots. BMC Plant Biology 2019;19(1):82.
[25] Beveridge TH, Li TS, Drover JC. Phytosterol content in American ginseng seed oil. Journal of Agricultural and Food Chemistry 2002;50(4):744–50.
[26] Tsugawa H, Cajka T, Kind T, Ma Y, Higgins B, Ikeda K, et al. MS-DIAL: data-independent MS/MS deconvolution for comprehensive metabolome analysis. Nature Methods 2015;12(6):523.
[27] Chong J, Soufan O, Li C, Caraus I, Li S, Bourque G, et al. MetaboAnalyst 4.0: towards more transparent and integrative metabolomics analysis. Nucleic Acids Res 2018;46(W1). W486-w94.
[28] Lopez-Ibanez J, Pazos F, Chagoyen M. MBROLE 2.0-functional enrichment of chemical compounds. Nucleic Acids Res 2016;44(W1):W201–4.
[29] Beveridge THJ, Li TSC, Drover JCG. Phytosterol content in American ginseng seed oil. Journal of Agricultural and Food Chemistry 2002;50(4):744–50.
[30] Lee M-H, Kim S-S, Cho C-W, Choi S-Y, In G, Kim K-T. Quality and characteristics of ginseng seed oil treated using different extraction methods. J Ginseng Res 2013;37(4):468–74.
[31] Takatsuto S. Brassinosteroids: distribution in plants, bioassays and microanalysts by gas chromatography—mass spectrometry. Journal of Chromatography A 1994;658(1):3–15.
[32] Qi J, Sun P, Liao D, Sun T, Zhu J, Li X. Transcriptomic analysis of American ginseng seeds during the dormancy release process by RNA-Seq. PloS One 2015;10(3):e0118558.
[33] Kim M-J, Shim C-K, Kim Y-K, Hong S-J, Park J-H, Han E-J, et al. Enhancement of seed dehiscence by seed treatment with Talaromyces flavus GG01 and GG04 in ginseng (Panax ginseng). The Plant Pathology Journal 2017;33(1):1.
[34] Yang D, Cheon S, Lee S, Yang D, Kim H. The effects of various dehiscence materials, growth regulators and fungicides on the ginseng seed. Korean J Ginseng Sci 1982;6:56–66.
[35] Kim YC, Kim YB, Park HW, Bang KH, Kim JU, Jo IH, et al. Optimal harvesting time of ginseng seeds and effect of gibberellic acid (GA 3) treatment for improving stratification rate of ginseng (Panax ginseng CA Meyer) seeds. Korean Journal of Medicinal Crop Science 2014;22(6):423–8.
[36] Lee JW, Nihhs R, Kim Y, Nihhs R, Kim J, Nihhs R, et al. Effects of gibberellic acid and alternating temperature on breaking seed dormancy of Panax ginseng CA Meyer. Korean Journal of Medicinal Crop Science 2016.
[37] Yang K, Yang L, Fan W, Long GQ, Xie SQ, Meng ZG, et al. Illumina-based transcriptomic analysis on recalcitrant seeds of Panax notoginseng for the dormancy release during the after-ripening process. Physiologia Plantarum 2018.
[38] Alemanno L, Berthouly M, Michaux-Ferriere N. A comparison between Theobroma cacao L. zygotic embryogenesis and somatic embryogenesis from floral explants. In Vitro Cellular & Developmental Biology-Plant 1997;33(3):163–72.
[39] Baud S, Boutin J-P, Miquel M, Lepiniec L, Rochat C. An integrated overview of seed development in Arabidopsis thaliana ecotype WS. Plant Physiology and Biochemistry 2002;40(2):151–60.
[40] Li J, Wang C, Han X, Qi W, Chen Y, Wang T, et al. Transcriptome analysis to identify the putative biosynthesis and transport genes associated with the medicinal components of Achyranthes bidentata Bl. Frontiers in Plant Science 2016;7:1860.
[41] Kim Y-K, Kim YB, Uddin MR, Lee S, Kim S-U, Park SU. Enhanced triterpene accumulation in Panax ginseng hairy roots overexpressing mevalonate-5-pyrophosphate decarboxylase and farnesyl pyrophosphate synthase. ACS Synthetic Biology 2014;3(10):773–9.
[42] Neelakandan AK, Nguyen HTM, Kumar R, Tran L-SP, Guttikonda SK, Quach TN, et al. Molecular characterization and functional analysis of Glycine max sterol methyl transferase 2 genes involved in plant membrane sterol biosynthesis. Plant Molecular Biology 2010;74(4):503–18.
[43] Vriet C, Russinova E, Reuzeau C. From squalene to brassinolide: the steroid metabolic and signaling pathways across the plant kingdom. Molecular Plant 2013;6(6):1738–57.
[44] Choi D-W, Jung J, Im Ha Y, Park H-W, In DS, Chung H-J, et al. Analysis of transcripts in methyl jasmonate-treated ginseng hairy roots to identify genes involved in the biosynthesis of ginsenosides and other secondary metabolites. Plant Cell Reports 2005;23(8):557–66.
[45] Kim Y-S, Han J-Y, Lim S, Choi Y-E. Ginseng metabolic engineering: regulation of genes related to ginsenoside biosynthesis. Journal of Medicinal Plants Research 2009;3(13):1270–6.
[46] Lee M-H, Jeong J-H, Seo J-W, Shin C-G, Kim Y-S, In J-G, et al. Enhanced triterpene and phytosterol biosynthesis in Panax ginseng overexpressing squalene synthase gene. Plant and Cell Physiology 2004;45(8):976–84.
[47] Sivakumar G, Yu K, Paek K. Enhanced production of bioactive ginsenosides from adventitious roots of Panax ginseng in bioreactor culture. J Hortic Sci Biotechnol 2006;81(3):549–52.
[48] Noguchi T, Fujioka S, Choe S, Takatsuto S, Tax FE, Yoshida S, et al. Biosynthetic pathways of brassinolide in Arabidopsis. Plant Physiology 2000;124(1):201–10.
[49] Hartmann M-A. Plant sterols and the membrane environment. Trends in Plant Science 1998;3(5):170–5.
[50] Schaller H. The role of sterols in plant growth and development. Progress in Lipid Research 2003;42(3):163–75.
[51] Zhou W, Branch WD, Gilliam L, Marshall JA. Phytosterol composition of Arachis hypogaea seeds from different maturity classes. Molecules 2018;24(1):106.
[52] Ferrer A, Altabella T, Arró M, Boronat A. Emerging roles for conjugated sterols in plants. Progress in Lipid Research 2017;67:27–37.
[53] Clouse SD. Brassinosteroid signal transduction: from receptor kinase activation to transcriptional networks regulating plant development. The Plant Cell 2011;23(4):1219–30.
[54] Divi UK, Krishna P. Brassinosteroid: a biotechnological target for enhancing crop yield and stress tolerance. New Biotechnology 2009;26(3–4):131–6.
[55] Vriet C, Russinova E, Reuzeau C. Boosting crop yields with plant steroids. The Plant Cell 2012;24(3):842–57.
[56] Kour J, Kohli SK, Khanna K, Bakshi P, Sharma P, Singh AD, et al. Brassinosteroid signaling, crosstalk and, physiological functions in plants under heavy metal stress. Frontiers in Plant Science 2021;12(204).
[57] Peres ALGL, Soares JS, Tavares RG, Righetto G, Zullo MAT, Mandava NB, et al. Brassinosteroids, the sixth class of phytohormones: a molecular view from the discovery to hormonal interactions in plant development and stress adaptation. International Journal of Molecular Sciences 2019;20(2):331.
[58] Planas-Riverola A, Gupta A, Betegón-Putze I, Bosch N, Ibañes M, Caño-Delgado AI. Brassinosteroid signaling in plant development and adaptation to stress. Development 2019;146(5):dev151894.
[59] Kim Y-H, Ahn I-O, Khan AL, Kamran M, Waqas M, Lee J-S, et al. Regulation of endogenous gibberellins and abscisic acid levels during different seed collection periods in Panax ginseng. Horticulture, Environment, and Biotechnology 2014;55(3):166–74.